

# Vessel Extraction in Retinal Images using Multilevel Line Detection

S. Rattathanapad, P. Mittrapiyanuruk, P. Kaewtrakulpong, B. Uyyanonvara, and C. Sinthanayothin

**Abstract**— This paper presents an algorithm to segment the blood vessels in retinal images. The contribution of this work is that we exhibit how a line detection can be applied in a multi-scale framework to fulfill the sophisticated task of vessel segmentation. The key idea of our algorithm is to systematically combine the outputs of Gaussian based line detection that is applied sequentially to the input image at several scales from coarse to fine levels. This brings down to the strategy that the evidences of smaller vessels are used to steer the process of addition of larger size vessels. Our proposed method is evaluated on the public DRIVE database and shows results with false positive rate.

## I. INTRODUCTION

THE blood vessels in a retinal image is an important indicator for diagnosing some diseases such as diabetes, hypertension, and arteriosclerosis. Typically ophthalmologists use the characteristics of vessels e.g. caliber, color, tortuosity to diagnose and plan a treatment for patients. The images, for example in Fig. 1, taken from retinal cameras are usually unevenly, non-uniformly illuminated, and poorly contrast. This could make an ophthalmologist take a lot of time to diagnose. To ease this process, many algorithms were developed to segment blood vessels in retinal images.

The techniques in the current state-of-the-art can be roughly divided into two major categories, namely supervised method and unsupervised method. For the first one [1], [2], the methods are based on supervised machine learning techniques in which each image pixel will be classified as either vessel or non-vessel. For the unsupervised category, several techniques are proposed. In [3], [4] the authors proposed the methods using mathematical morphology. In [5], [6] the methods based on vessel tracking are presented. In [7], the combination of a

graph-theoretical algorithm with vessel tracking technique is proposed. In [8], [9] the authors proposed the methods based on matched filtering techniques.

The remaining of this paper is organized as follows. In Section 2, we summarize the line detection algorithm used in this work. Then, our proposed method is presented in Section 3. The experimental results and discussion are presented in Section 4. Finally, the conclusion is drawn.

## II. LINE DETECTION

In our algorithm, we use the line detection method proposed by C. Steger [10]. In this section we will give a concise review of the line detection method. For more details, we encourage the reader to consult the materials presented in [10].

In Steger's method, an explicit model is used to characterize the lines and their surroundings. Then the detection algorithm is derived from the analysis of the scale-space behavior of the model line profile. This turns out into the detection algorithm that use the differential geometric functions computed from the image. The line points are defined on the image pixels that have vanishing gradients and high curvature in the direction perpendicular to the line.

In summary, the algorithm to detect lines with sub-pixel accuracy consists of the following steps:

- (1) Convolve the image with discrete 2D Gaussian partial derivative kernel (see the equation in [10]) where  $\sigma$  is the kernel smoothing parameter. This give us, at any point  $(x, y)$  in the image, the partial derivatives  $r_x, r_y, r_{xy}, r_{xx},$  and  $r_{yy}$ .
- (2) For each image point  $(x, y)$ ,

- (2.1) Compute the eigenvalues and eigenvectors of the following Hessian matrix (1)

$$H(x, y) = \begin{pmatrix} r_{xx} & r_{xy} \\ r_{xy} & r_{yy} \end{pmatrix} \quad (1)$$

We denote  $(n_x, n_y)$  to be the eigenvector corresponding to the eigenvalue of maximum absolute value.

- (2.2) Compute  $(p_x, p_y)$  by (2)

$$(p_x, p_y) = (tn_x, tn_y) \quad (2)$$

Where

$$t = -\frac{r_x n_x + r_y n_y}{r_{xx} n_x^2 + 2r_{xy} n_x n_y + r_{yy} n_y^2} \quad (3)$$

- (2.3) if  $(p_x, p_y) \in \left[-\frac{1}{2}, \frac{1}{2}\right] \times \left[-\frac{1}{2}, \frac{1}{2}\right]$  and the second directional derivative along  $(n_x, n_y)$  is larger than a threshold,

Manuscript received November 8, 2011. This work was supported by the Higher Education Research Promotion and National Research University Project of Thailand, Office of the Higher Education Commission, TAIST, NSTDA, Tokyo Institute of Technology and SIIT.

F. S. Rattathanapad is with the Department of ICT, Sirindhorn International Institute of Technology, Thammasat University, Thailand (e-mail: [suthit@siit.tu.ac.th](mailto:suthit@siit.tu.ac.th)).

S. P. Mittrapiyanuruk is with the Department of Mathematics, Srinakharinwirot University, Thailand (e-mail: [praditm@swu.ac.th](mailto:praditm@swu.ac.th)).

T. P. Kaewtrakulpong is with Department of Control Systems and Instrumentation Engineering, King Mongkut's University of Technology Thonburi, Thailand (e-mail: [pakorn.kae@kmutt.ac.th](mailto:pakorn.kae@kmutt.ac.th)).

F. B. Uyyanonvara is with Department of ICT, Sirindhorn International Institute of Technology, Thammasat University, Thailand (e-mail: [bunyarit@siit.tu.ac.th](mailto:bunyarit@siit.tu.ac.th)).

F. C. Sinthanayothin is with National Electronics and Computer Technology Center, NSTDA, Thailand (e-mail: [chanjira.sinthanayothin@nectec.or.th](mailto:chanjira.sinthanayothin@nectec.or.th)).

we declare the point  $(x, y)$  as a line point where  $(p_x, p_y)$  is the sub-pixel location of the point.

(3) Construct a set of line primitives by grouping a set of line pixels that share the same curvilinear structure. Each line primitive is specified with two end points and the set of points belonging to the line.

To apply the aforementioned method to our algorithm, we apply a collection of line detectors by varying the smoothing parameter, i.e., that results in multiple corresponding sets of line points. Then we devise an algorithm (presented in the next section) to combine these set of points into the single result of vessel extraction.

### III. METHOD

The motivation behind our algorithm is based on the following observations of vessel characteristics. That is, the vessel typically spreads itself out of the optic disc in a tree-like manner. As the portions of vessels branch out of their parents, the calibers of vessels are gradually decreasing. An example of the aforementioned characteristics can be seen in Fig. 1.

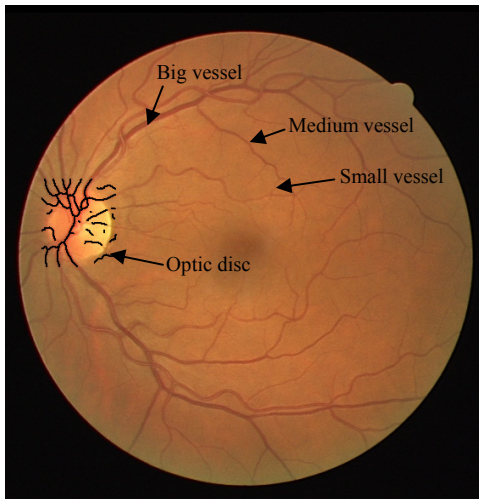


Fig. 1 The first retinal image in DRIVE database.

Basically, the larger vessels can be segmented with more reliability than the smaller ones. With regard to line detection, larger vessels can be detected with a large Gaussian smoothing parameter. Meanwhile the smaller values are used to extract tiny vessels with the cost of boosting high frequency noises into the result. An example of this effect can be shown in Fig. 2 where a collection of line detections with  $\sigma = 4, 3.5, \dots, 1.5$  is applied to the image. Therefore, as mentioned previously, the small vessels must connect to large vessels at some particular points. This information is useful to separate the actual small vessels from the noise portions.

Based on this observation we design the algorithm to incrementally extract the vessels and add to the larger vessels extracted earlier. The criteria to connect these vessels are derived from the local image characteristics of

vessel portions e.g. proximity, orientation, and gradient.

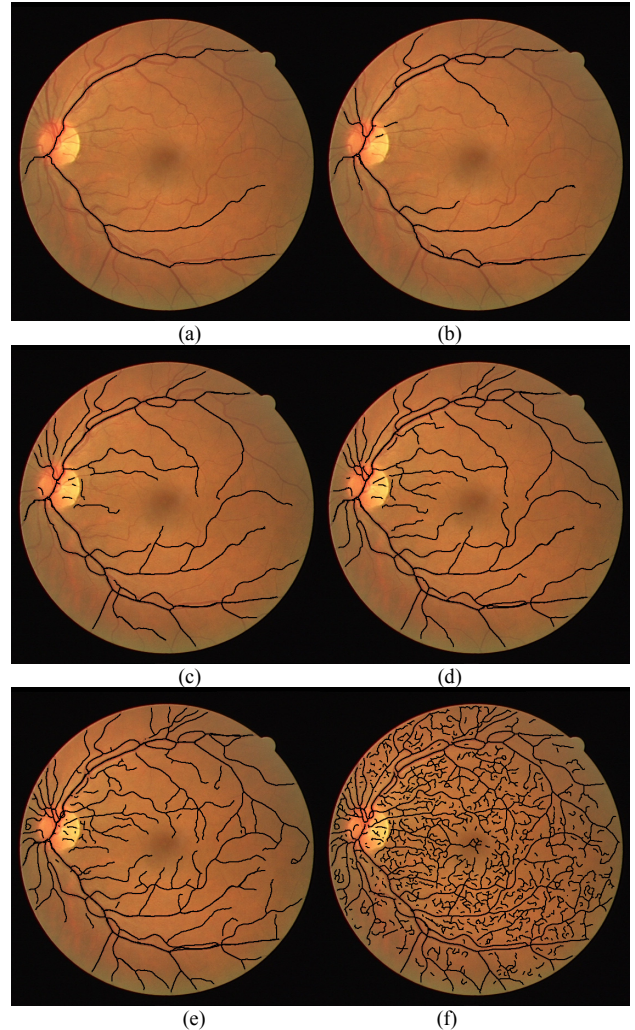


Fig. 2 Line detection with (a)  $\sigma = 4.0$ , (b)  $\sigma = 3.5$ , (c)  $\sigma = 3.0$ , (d)  $\sigma = 2.5$ , (e)  $\sigma = 2.0$ , (f)  $\sigma = 1.5$

The pseudo-code of our algorithm can be shown in table I in which the details can be explained as follows:

Step 1: We extract the vessels in the vicinity of optic disc region. Currently we require a user to interactively specify the region of interest (ROI) of the optic disc. In the future, we plan to use an automatic optic disc localization method such as the one in [13] to accomplish this task. Next we create a crop image from the input image within ROI and then we apply the line detection with  $\sigma = k\sigma_i$  where  $\sigma_i$  is the starting value of Gaussian Smoothing parameter. In the experiment we set  $\sigma_i = 4$  and  $k = 0.5$ . The output of line detection is the list of x-y coordinates corresponding to line points. For the purpose of the connection explained next, each point is associated with the gradient magnitude and orientation. The set of line point extracted in the optic disc area will be used as the seed set to generate the final result ( $L_{out}$ ).

TABLE I  
Pseudo-code

```

V = VesselExtraction (I,  $\sigma_i$ ,  $\sigma_f$ ,  $\Delta$ , k)
Input: I = retinal image
Output: V = set of line points corr. to the vessel
Parameters:
 $\sigma_i$  = the initial value of Gaussian Smoothing parameter
 $\sigma_f$  = the final value of Gaussian Smoothing parameter
 $\Delta$  = step size
k = multiplicative constant
begin
roi  $\leftarrow$  interactively specify the optic disc region
Iimp = CropImage (I, roi)
Lout =  $\phi$ 
L = LineDetection (Iimp, k  $\sigma_i$ )
Lout = Lout  $\cup$  L
 $\sigma$  =  $\sigma_i$ 
while  $\sigma \geq \sigma_f$ 
L = LineDetection (I,  $\sigma$ )
Lout = Connection (Lout, L)
Limp = FindIsolatedVessel (L)
Lout = Lout  $\cup$  Limp
 $\sigma$  =  $\sigma - \Delta$ 
endwhile
V = Lout
end

```

Step 2: We iteratively apply the line detection to whole image in which the value of  $\sigma$  is initially set to  $\sigma_i$  and is decreased in each iteration with the value of  $\Delta$  until  $\sigma < \sigma_f$ . In this work we set  $\sigma_f = 1.5$ . The output of line detection at the current iteration will be combined into the final result ( $L_{out}$ ) by the “connection” function.

#### Step 2.1: Line curve connection

The main task of the “connection” is to determine whether a line primitive of the current level line detection result should be combined to line primitives in  $L_{out}$ . The key idea is adapted from [11]. The criteria to merge any two line primitives are based on the properties of the end points of both primitives. These include (i) end point distance, (ii) angle distance, (iii) connectivity distance, and (iv) gradient difference. We connect the line primitives if all of the above conditions are satisfied. The details of these criteria are presented as follows.

In Fig. 3(a), the end point distance is defined as Euclidean distance, in pixels, between the end point  $A$  and the end point  $B$ . This condition is satisfied when the distance is within a specified range.

Angle distance is defined as the difference between the angles of two line primitives. In Fig. 3(b), we demonstrate how to compute this value between the angle  $A$  and  $B$ . Similarly this condition is satisfied when the value is less than a threshold.

Connectivity distance is determined by projecting the end point of one curve as a line and finding the minimum distance from the projected line to the other endpoint. This condition is used only for the case of connecting more than two line primitives. If the distance to the projection from either endpoint is within a specified range, the condition is

satisfied. In Fig. 3(c), we show an example how to compute this distance between the end points of three line primitives. The distance between the end point  $A$  and the end point  $B$  is closer than the distance between the end point  $A$  and the end point  $C$ . However the connectivity distance will favor the end point  $A$  to connect to the end point  $C$  instead of the end point  $B$ .

Gradient difference is calculated by first determining the gradient angle at each end point, then taking the absolute difference of the two angles in degrees. And the condition is satisfied if the difference is less than a threshold. In Fig. 3(d) we show an example of the gradient angles of two line primitives that are totally opposite. In this case, the condition is not satisfied.

#### Step 2.2 Isolated vessel extractions

In this step we extract the vessels that are not combined to the final result ( $L_{out}$ ) recently. These vessels are considered as noise parts by the connection module. The gradient magnitudes of line points corresponding to these vessels are significantly high. However, the locations of these vessels are far from the ones of the current lists of final result ( $L_{out}$ ) that fails to the criteria of connection. To get around this problem any line primitive whose average gradient magnitude is greater than a threshold will be added into  $L_{out}$ .

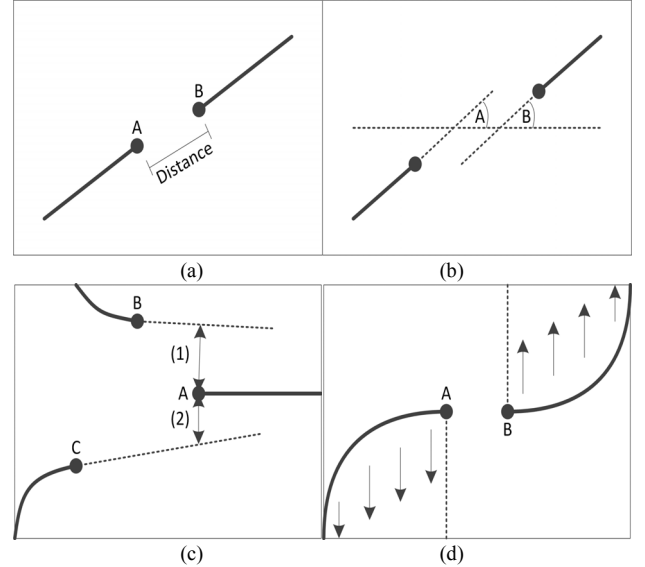


Fig. 3 The connection criteria (a) end points distance, (b) angle distance, (c) connectivity distance, and (d) gradient difference.

## IV. RESULT AND DISCUSSION

Our proposed method is evaluated on public DRIVE database [12]. DRIVE is a database assembled in The Netherlands, and it includes 40 fundus images of 584 x 565 pixels, captured using a 45° field-of-view fundus camera.

We show the performance of our algorithm with qualitative results in Fig. 4. The pictures in the first column show the results from our method. While the picture on next column show the same results plotting on the groundtruth

images. Our proposed method can detect most of the major part of vessel skeleton. In Fig. 6 we show the result of vessel extraction in each iteration of working. This shows the effectiveness of how the connection module can combine the vessels extracted at different levels of line detection into the final result.

In the future, we plan to tackle the problem of non-uniformly illuminated condition. An example of this effect is shown in Fig. 5(a). With the proposed algorithm in this paper the result is shown in Fig. 5(b). As you may observe, several false positive results are detected shown by the black circle area. One potential solution to this problem is to incorporate some contrast model or illumination model into the proposed method.

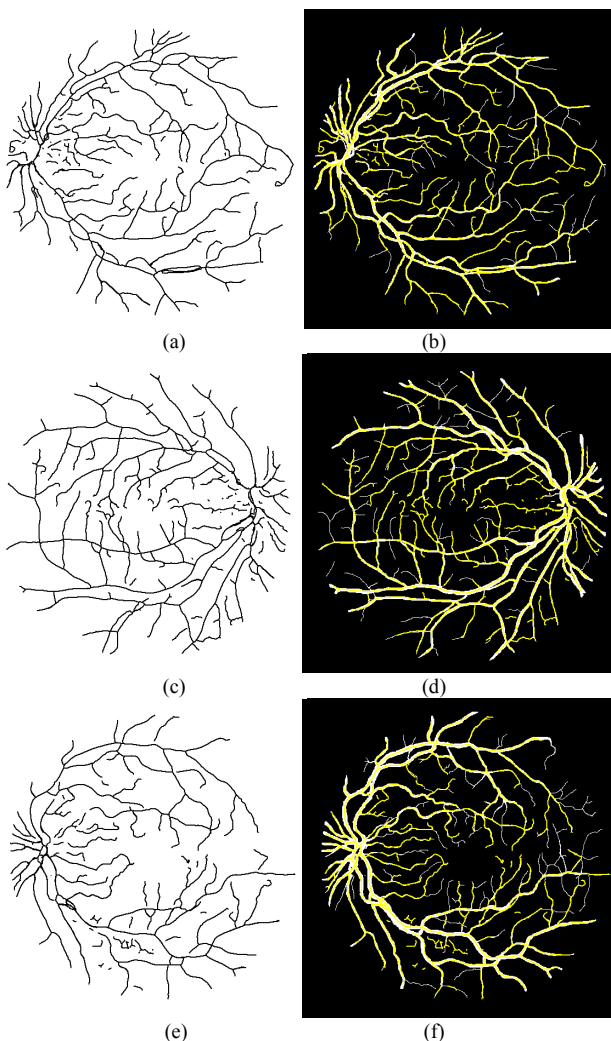


Fig. 4 the first column is the result our proposed method and the second column is the result plotting on groundtruth.

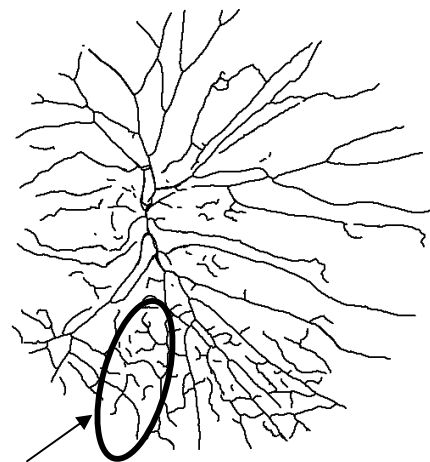
## V. CONCLUSION

In this paper, we present an algorithm to segment the blood vessel in retinal images. The algorithm is based on multilevel line detection and connection of line primitives.

Multilevel line detection is used for extracting the vessels at several values of Gaussian smoothing parameters. Then the line primitives extracted at different levels are connected into the single vessel extraction result.



(a)



(b)

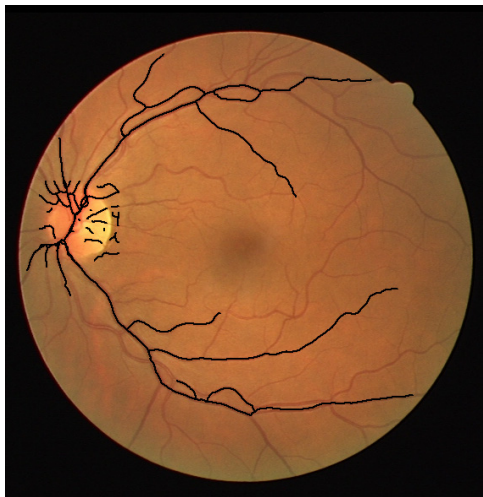
False positive

Fig. 5 (a) retinal image with non-uniformly illuminated, (b) resulting our proposed method.

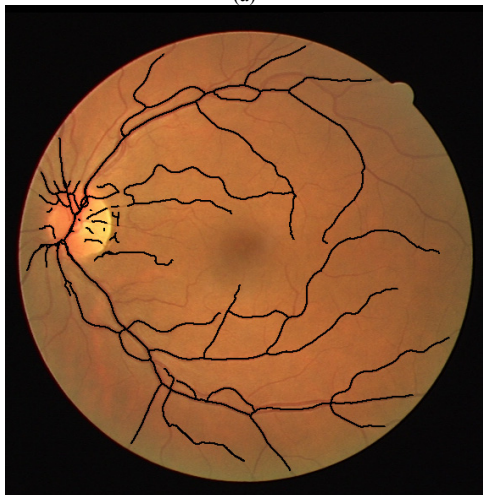
## REFERENCES

- [1] C. A. Lupascu, "FABC: Retinal Vessel Segmentation Using AdaBoost," *Information Technology in Biomedicine, IEEE Transactions*, vol. 14, pp. 1267-1274, 2010.
- [2] Sinthanayothin C, "Automated localization of the optic disc, fovea, and retinal blood vessels from digital color fundus images," *British Journal Ophthalmology*, 1999, vol. 83, pp. 902-910.
- [3] F. Zana, "Segmentation of vessel-like patterns using mathematical morphology and curvature evaluation," *IEEE Transactions on Image Processing* 10(7), pp. 1010-1019, 2001.
- [4] D. Welfer, "Segmentation of the optic disk in color eye fundus images using an adaptive morphological approach," *Computers in Biology and Medicine*, vol. 40, pp. 124-137, 2010.
- [5] E. Grisan, et al.: "A new tracking system for the robust extraction of retinal vessel structure," *Engineering in Medicine and Biology Society, 2004. IEMBS '04. 26th Annual International Conference of the IEEE*, pp. 1620-1623, 2004.

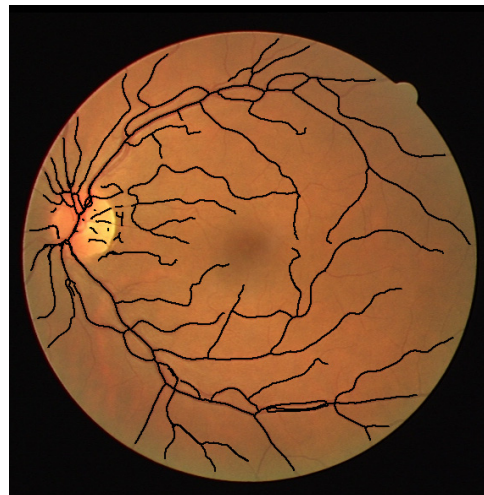
- [6] T. Yedidya, "Tracking of Blood Vessels in Retinal Images Using Kalman Filter," *Computing: Techniques and Applications, 2008. DICTA '08. Digital Image*, pp. 52-58, 2008.
- [7] S. Rattathanapad, "Vessel Segmentation in Retinal Images using Graph-Theoretical Vessel Tracking," *MVA2011 LAPR Conference on Machine Vision Applications*, pp. 548-551, 2011.
- [8] Sofka M, "Retinal vessel centerline extraction using multiscale matched filters, confidence and edge measures," *IEEE Transactions on Medical Imaging 25(12)*, pp. 1531-1546, 2006.
- [9] Al-Rawi M, "An improved matched filter for blood vessel detection of digital retinal images," *Computers in Biology and Medicine 37(2)*, pp. 262-267, 2007.
- [10] C. Steger: "An Unbiased Detector of Curvilinear Structures". *IEEE Transactions on Pattern Analysis and Machine Intelligence*, vol. 20, no. 2, pp. 113-125, 1998.
- [11] National Instruments, *Contour Extraction Concept* (NI Vision Concept Help), 2000
- [12] J. Staal, "Ridge-based vessel segmentation in color images of the retina," *Medical Imaging, IEEE Transactions*, vol. 23, pp. 501-509, 2004.
- [13] A. E. Mahfouz and A. S. Fahmy, "Ultrafast optic disc localization using projection of image features," in *Image Processing (ICIP), 2009 16th IEEE International Conference on*, 2009, pp. 665-668.



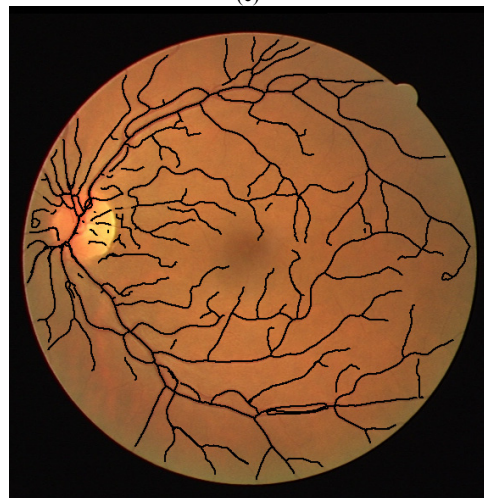
(a)



(b)



(c)



(d)

Fig. 6 Result image iteration (a) round 1, (b) round 2, (c) round 3, and (d) round 4